# A constitutive model for North Sea Chalk. Application to reservoir compaction and to waterflooding.

R.Charlier, F.Collin, C.Schroeder & P.Illing
*Département GéomaC, University of Liège, Belgium*

P.Delage, Y.J.Cui & V.De Gennaro
*CERMES, Ecole Nationale des Ponts et Chaussées, France*

ABSTRACT: Subsidence of chalk oil reservoirs in North Sea is related to the chalk compaction induced by fluid depletion and by the water – chalk interaction. A constitutive model is developed in order to take into account these two effects. It is based on frictional – cap elastoplasticity and on the Barcelona unsaturated soil model. Oil – water – chalk interaction is modeled through the suction variable. The two saturating fluids flow is also developed. After implementation into a finite element code, these tools allow to simulate a waterflooding experiment on a chalk sample. The model appears to reproduce qualitatively and quantitatively the experimental results.

## 1 INTRODUCTION

The compaction of chalky reservoirs during oil extraction and other important problems like the "casing collapse" or the "chalk production" are related to the *mechanical properties of chalk*. Controlling compaction is very important because reservoir deformations imply seabed subsidence that endangers the offshore stations.

The first explanation of subsidence related the compaction to the pore pressure decrease in the reservoir. The solution was the injection of gas and water into the oilfield in order to repressurise the reservoir. But the waterflooding induced additional subsidence. Though many studies have been already performed on chalks, the basis mechanism of the water sensitivity was not defined. Obviously, no satisfactory constitutive law can be written without this deep insight of the phenomenon. This is the scope of the ongoing EC Research Program ***Pasachalk***. The origin of the research is in the comparison of experimental results obtained on Lixhe chalk and on Jossigny silt which showed that the influence of water on pure high porosity chalk is similar to that on partially saturated soils (Delage & al. 1996). Another extensive experimental analysis of the influence of the saturating fluid on Lixhe chalk behaviour concluded that the water-weakening effect might be suction related. Hence the idea appeared to apply the knowledge, the approach, and the tools of the partially saturated soil mechanics to the understanding, description, and modelling of chalk behaviour during changes in saturation fluids, such as when waterflooding.

This paper presents the developed constitutive model, which is a cap type plasticity model coupled with the Barcelona one (Alonso & al. 1990) for taking the suction effect into account.

The model parameters are calibrated based on the experimental results. The validation of the model is performed on a waterflooding experiment. We show that the model is able to reproduce qualitatively and quantitatively the observed basic phenomena.

## 2 CONSTITUTIVE MODELS

Experiments performed on chalk samples have shown two plastic mechanisms: the pore collapse for high mean stresses (contractant behaviour) and the frictional failure for low mean stresses. The pore collapse could be caused by the breakdown of physico-chemical bonds between the grains inducing some grain-to-grain slip (Monjoie & al. 1990). The frictional failure corresponds to a plastic distortion inducing an increase of porosity.

The two evidenced plastic mechanisms are modeled by two yield surfaces combined within a cap model: the modified Cam-Clay model is used for pore collapse whereas an internal friction model for friction failure. Experimental results show that the chalk strength under extension can be overestimated using an internal friction model, a third yield surface is then adopted to limit traction stresses.

Obviously, the so defined yield curve is not continuously derivable at the intersections, leading to numerical difficulties. However, recent publications

provided an elegant way to solve this problem (Simo & Hugues, 1998).

As far as the suction effect is concerned, the model adopts the approach developed in the Barcelona Basic Model (Alonso & al. 1990) where the suction is considered as an independent variable. Suction modifies yield surfaces and produces reversible and irreversible deformations.

Moreover, two fluids flow model is also presented, in order to be able to analyse fully coupled problems. The multi-phase flow model is based on works in relation with the problem of nuclear waste disposal (Collin & al. 2001).

## 2.1 *Mechanical model*

The mechanical model is expressed in terms of the following stress invariants and the suction:

$$I_\sigma = \sigma_{ii} \tag{1}$$

$$II_{\hat{\sigma}} = \sqrt{\frac{1}{2}\hat{\sigma}_{ij}\hat{\sigma}_{ij}}\,,\ \hat{\sigma}_{ij} = \sigma_{ij} - \frac{I_\sigma}{3}\delta_{ij} \tag{2}$$

$$III_{\hat{\sigma}} = \frac{1}{3}\hat{\sigma}_{ij}\hat{\sigma}_{jk}\hat{\sigma}_{ki} \tag{3}$$

$$\beta = -\frac{1}{3}\sin^{-1}\left(\frac{3\sqrt{3}}{2}\frac{III_{\hat{\sigma}}}{II_{\hat{\sigma}}{}^3}\right) \tag{4}$$

$$s = p_o - p_w \tag{5}$$

Where $\beta$ is the Lode angle, $s$ is the suction, $p_o$ and $p_w$ are the oil and water pressures.

### 2.1.1 *General formulation*

The general elastoplastic relations are formulated in rate form. The strain rate is composed of a mechanical part (superscript *m*) and of suction one (superscript *s*). Each contribution is partitioned in an elastic (superscript *e*) and a plastic component (superscript *p*):

$$\dot{\varepsilon}_{ij} = \dot{\varepsilon}_{ij}^{m,e} + \dot{\varepsilon}_{ij}^{s,e} + \dot{\varepsilon}_{ij}^{m,p} + \dot{\varepsilon}_{ij}^{s,p} \tag{6}$$

The mechanical elastic part is related to the Jaumann objective stress rate through Hooke's law:

$$\tilde{\sigma}_{kl} = C_{klij}^e \dot{\varepsilon}_{ij}^{m,e} \tag{7}$$

Where $\boldsymbol{C}^e$ is the compliance elastic tensor.

For the plastic parts, a general framework of non-associated plasticity is adopted in order to limit dilatancy. In that case, the plastic flow rate is derived from a plastic potential $g_\alpha$:

$$\dot{\varepsilon}_{ij}^{m,p} = \dot{\lambda}^p \frac{\partial g_\alpha}{\partial \sigma_{ij}}\,, \tag{8}$$

where $\lambda^p$ is a scalar multiplier and $g_\alpha$ is the plastic potential related to the plastic mechanism $\alpha$.

Elastic and plastic deformations related to suction changes are defined following expressions given in Barcelona Basic Model. Irreversible deformations are induced when the suction becomes higher than a suction level $s_0$.

$$\dot{\varepsilon}_{ij}^{s,e} = \frac{\kappa_s}{(1+e)}\frac{\dot{s}}{(s+p_{at})}\delta_{ij} = h_{ij}^e \dot{s} \tag{9}$$

$$\dot{\varepsilon}_{ij}^{s,p} = \frac{\lambda_s - \kappa_s}{(1+e)}\frac{\dot{s}}{(s+p_{at})}\delta_{ij} = h_{ij}^p \dot{s} \tag{10}$$

Where $e$ is the void ratio, $p_{at}$ is the atmospheric pressure, $\kappa_s$ and $\lambda_s$ are elastic and plastic coefficients.

The equations (6) and (7) can be rewritten as:

$$\tilde{\sigma}_{kl} = C_{klij}^e\left(\dot{\varepsilon}_{ij} - h_{ij}^e\dot{s} - \dot{\lambda}^p\frac{\partial g_\alpha}{\partial \sigma_{ij}} - h_{ij}^p\dot{s}\right) \tag{11}$$

Considering a general hardening/softening plastic law depending on the internal variable $\zeta$, the consistency condition related to the yield function $f_\alpha$ can be formulated as:

$$\dot{f}_\alpha = \frac{\partial f_\alpha}{\partial \sigma_{ij}}\tilde{\sigma}_{ij} + \frac{\partial f_\alpha}{\partial s}\dot{s} + \frac{\partial f_\alpha}{\partial \zeta}\dot{\zeta} = 0 \tag{12}$$

Substituting (11) in (12), the expression of multiplier $\lambda^p$ can be found and the stress rate can be computed:

$$\tilde{\sigma}_{kl} = (C_{klij}^e - C_{klij}^p)\dot{\varepsilon}_{ij} - M_{kl}\dot{s} \tag{13}$$

The first term of the right part is the classical expression of an elastoplastic formulation. The second term is related to the suction.

### 2.1.2 *CamClay model*

The Cam-Clay yield surface is defined by the following expression:

$$f_1 \equiv II_{\hat{\sigma}}^2 + m^2\left(I_\sigma + \frac{3c}{tan\,\phi_C}\right)(I_\sigma - 3p_0) = 0 \tag{14}$$

Where $c$ is the cohesion, $\phi_C$ is the friction angle in compression path, $p_0$ is the preconsolidation pressure, which defines the size of the yield surface, and $m$ is a coefficient introduced to take into account the effect of the third stress invariant.

The coefficient $m$ is defined by:

$$m = a(1 + b\,sin\,3\beta)^n \tag{15}$$

where the parameters $a$, $b$ and $n$ must verify some convexity conditions (Van Eekelen 1980).

The plastic flow is supposed to be associated and the internal variable is the pre-consolidation pressure $p_0$, which is related to the volumetric plastic deformations $d\varepsilon_v^p$ following the kinematic equation:

$$dp_0 = \frac{1+e}{\lambda-\kappa} p_0 d\varepsilon_v^p , \tag{16}$$

where $\lambda$ is the compression coefficient and $\kappa$ is the elastic coefficient.

Using this relation, either hardening or softening could appear according to the sign of the volumetric plastic deformations. However, in the cap model, the softening zone will not be considered.

2.1.3 *Internal friction model*

A more sophisticated model can be built from the Drucker-Prager's cone by introducing a dependence on the Lode's angle $\beta$, in order to match more closely the Mohr-Coulomb criterion. It consists of a smoothed Mohr-Coulomb plasticity surface. The formulation based on the idea of Van Eekelen (1980) is used. It can be written in a very similar way to the Drucker-Prager's criterion:

$$f_2 \equiv II_{\hat{\sigma}} - m\left( I_\sigma + \frac{3c}{tan\phi_C} \right) = 0 \tag{17}$$

A non-associated plasticity is considered here using a plastic potential definition similar to Eq. 17 where the dilatancy angle $\psi$ is used instead of the frictional angle.

The internal variables of the model are the frictional angles $\phi_C$ (for compression paths), $\phi_E$ (for extension paths) and the cohesion $c$. The following hardening relations are defined using the plastic equivalent deformations:

$$\begin{aligned} \phi_C &= \phi_{C0} + \frac{(\phi_{Cf} - \phi_{C0})\varepsilon_{eq}^p}{B_p + \varepsilon_{eq}^p} \\ \phi_E &= \phi_{E0} + \frac{(\phi_{Ef} - \phi_{E0})\varepsilon_{eq}^p}{B_p + \varepsilon_{eq}^p} \\ c &= c_0 + \frac{(c_f - c_0)\varepsilon_{eq}^p}{B_c + \varepsilon_{eq}^p} \end{aligned} \tag{18}$$

where subscripts 0 and $f$ mean the initial and the final value respectively; $B_p$ and $B_c$ are parameters defining the plastic deformation for which half of the internal variable hardening is achieved.

The equivalent plastic strain represents the cumulated equivalent or deviatoric plastic strains du-ring time $t$:

$$\varepsilon_{eq}^p = \int_0^t \dot{\varepsilon}_{eq}^p dt , \tag{19}$$

2.1.4 *Suction effect on yield surface*

Several phenomena are usually evidenced for unsaturated soils:

1. The preconsolidation pressure $p_0$ and the material stiffness increase with suction. This is described by the LC concept of the Barcelona model:

$$p_0(s) = p_c \left( \frac{p_0^*}{p_c} \right)^{\frac{\lambda(0)-\kappa}{\lambda(s)-\kappa}} \tag{20}$$

with

$$\lambda(s) = \lambda(0)\left[(1-r)exp(-\beta' s) + r\right] \tag{21}$$

where $p_0^*$ is the preconsolidation pressure for $s = 0$, $p_c$ is a reference pressure, $\lambda(0)$ is the compression coefficient at zero suction, $\lambda(s)$ is the compression coefficient at suction $s$, $r$ is a parameter representing the maximum stiffness of the chalk, and $\beta'$ is a parameter controlling the stiffness increase with suction increase.

2. Cohesion increases with suction, this is modelled using Eq. 22. The influence of suction on friction angle depends on the material studied. Experiment on chalk shows that friction angle is independent of the saturating fluid.

$$c(s) = c(0) + k\, s \tag{22}$$

where $k$ is a material constant, $c(0)$ is the cohesion at saturated state.

3. Suction changes may create irreversible strains. In the Barcelona model, this is modelled thanks a yield surface, the SI "Suction Increase" curve. When suction becomes higher than a suction level $s_0$, plastic strains are created. This yield criterion is introduced in our constitutive law:

$$f_4 \equiv s - s_0 = 0 \tag{23}$$

Figure 1 presents all the yield surfaces in the stress space.

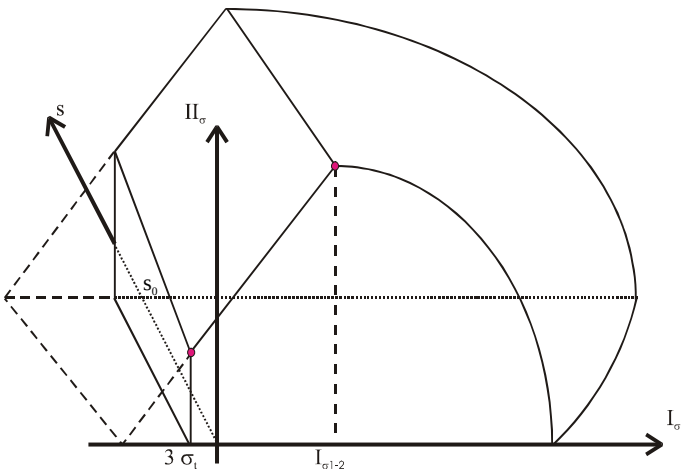

Figure 1: Cap model in the stress space

## 2.2 *Numerical law integration*

The existence of four yield surfaces in the model leads to complex law integration. One has not only to determine which plastic mechanism is active, but also to manage the case where two surfaces are active. This case occurs at the intersection of two surfaces: the apex regime is a combination of two mechanisms.

Integration over time of the general rate constitutive elastoplastic relation (13) leads to the incremental form:

$$\Delta\sigma_{ij} = \left(C^{e}_{ijkl} - C^{p}_{ijkl}\right)\Delta\varepsilon_{kl} - M_{kl}\Delta s \tag{24}$$

The method used here is commonly based on the operator-split methodology (Simo & Taylor 1985), which consists in computing an elastic predictor/plastic corrector. The elastic predictor computed, one can determine the active plastic regime. This is important when the stress state is close to an apex. It must be mentioned that the notion of proximity is relative and arbitrary.

Hughes & Simo (1998) proposed a technique for integrating the law in an apex regime in accordance with which the following consistency conditions must be verified:

$$\begin{cases} f_1 = 0 \text{ and } f_2 = 0 \\ \dot{f}_1 = 0 \text{ and } \dot{f}_2 = 0 \end{cases} \tag{25}$$

$f_1$ and $f_2$ being the yield functions related to the plastic mechanisms 1 and 2, respectively.

The plastic strain is the sum of the plastic strains due to the mechanisms 1 and 2:

$$\dot{\varepsilon}^{p}_{ij} = \dot{\varepsilon}^{p,1}_{ij} + \dot{\varepsilon}^{p,2}_{ij} = \dot{\lambda}^{p,1}\frac{\partial g_1}{\partial\sigma_{ij}} + \dot{\lambda}^{p,2}\frac{\partial g_2}{\partial\sigma_{ij}} \tag{26}$$

Where $g_1$ and $g_2$ are the plastic potentials associated respectively to the plastic mechanisms 1 and 2.

Considering that yield surfaces ($f_\alpha$, $\alpha$ = 1, 2) are only function of the stress state ($\sigma_{ij}$), suction $s$ and hardening variables ($\zeta^\alpha$), the Taylor's series for consistency conditions (25) are given as:

$$\begin{aligned} &f_\alpha\left(\sigma_{ij} + \Delta\sigma^{p}_{ij}, s + \Delta s, \zeta^\alpha + \Delta\zeta^\alpha\right) \\ &= f_\alpha\left(\sigma_{ij}, s, \zeta^\alpha\right) + \frac{\partial f_\alpha}{\partial\sigma_{ij}}\Delta\sigma^{p}_{ij} + \frac{\partial f_\alpha}{\partial s}\Delta s + \frac{\partial f_\alpha}{\partial\zeta^\alpha}\Delta\zeta^\alpha \end{aligned} \tag{27}$$

With

$$\Delta\sigma^{p}_{ij} = -C^{e}_{ijkl}\Delta\left(\varepsilon^{p,1}_{kl} + \varepsilon^{p,2}_{kl}\right) \tag{28}$$

$$\Delta\zeta^\alpha = \frac{d\zeta^\alpha}{d\varepsilon^{p,\alpha}}\Delta\varepsilon^{p,\alpha} \tag{29}$$

The plastic strains can be expressed in a general form as:

$$\Delta\varepsilon^{p,\alpha} = \dot{\lambda}^{p} Val^\alpha \tag{30}$$

Where $Val^\alpha$ is a function of the plastic potential derivatives.

Using equations (26), (28) and (29), equation (27) can be re-written:

$$\begin{aligned} f_\alpha = f_\alpha\left(\sigma_{ij}, s, \zeta^\alpha\right) &- \frac{\partial f_\alpha}{\partial\sigma_{ij}} C^{e}_{ijkl}\left(\sum_{n=1}^{2}\Delta\lambda^{p,n}\frac{\partial g_n}{\partial\sigma_{kl}}\right) \\ &+ \frac{\partial f_\alpha}{\partial s}\Delta s + Val^\alpha\frac{\partial f_\alpha}{\partial\zeta^\alpha}\frac{d\zeta^\alpha}{d\varepsilon^{p,\alpha}}\Delta\lambda^{p,\alpha} \end{aligned} \tag{31}$$

Knowing that in the plastic regime $f = 0$, the previous relation gives an incremental consistency equation for each mechanisms.

The system of equations provides the value of the two plastic multiplicators, $\Delta\lambda^{p,1}$ and $\Delta\lambda^{p,2}$. When both values are positive, the two mechanisms are activated simultaneously, however, if one multiplicator is negative, the corresponding mechanism must not be activated, and the computation is reiterated only with the other yield surface.

## 2.3 *Diffusion model*

Unsaturated flow formulation used here is based on works in relation with the problem of nuclear waste disposal (Collin & al. 2001). For each fluid (Water and oil), balance equations and state equations are written. In partial saturation conditions, the permeability and the storage law have to be modified: a generalised Darcy's law defines the fluid motion (Bear 1972). Numerous couplings existing between mechanics and flows are considered.

### 2.3.1 *Water*

The generalised Darcy's law for multiphase porous medium gives liquid water velocity:

$$\underline{f}_w = -\frac{k_{r,w}k_{\text{int}}}{\mu_w}\left[\underline{grad}(p_w) + g\rho_w\underline{grad}(y)\right] \tag{32}$$

Where $f_w$ is water macroscopic velocity; $\rho_w$ is water density; $p_w$ is the liquid water pressure; $y$ is the vertical upward directed co-ordinate; $g$ is the gravity acceleration; $\mu_w$ is the dynamic viscosity of the liquid water; $k_{int}$ is the intrinsic permeability of the medium and $k_{r,w}$ is the water relative permeability which varies with respect to the saturation degree.

The balance equation includes the variation of water storage and the divergence of water flows:

$$\frac{\partial}{\partial t} f^{*}_{w} + div\left(\rho_w.\underline{f}_w\right) = 0 \tag{33}$$

where $t$ is the time and $f_w^*$ is the water storage:

$$f^{*}_{w} = \rho_w.n.S_{r,w} \tag{34}$$

with $n$ the porosity and $S_{r,w}$ the water saturation degree.

The water density is depending on water pressure according to:

$$\rho_w = \rho_{w,0}\left(1+\frac{p_w - p_{w,0}}{\chi_w}\right) \quad (35)$$

where $\rho_{w,0}$ is the water density at reference pressure $p_{w,0}$, $\rho_w$ is the density at pressure $p_w$ and $\chi_w$ is the water compressibility.

#### 2.3.2 *Oil*

Considering the generalised Darcy's law for multiphase porous medium, oil velocity is given by:

$$\underline{f}_o = -\frac{k_{r,o}k_{\text{int}}^{sat}}{\mu_o}.\left[\underline{grad}(p_o) + g.\rho_o.\underline{grad}(y)\right] \quad (36)$$

Where $f_o$ is oil macroscopic velocity; $\rho_o$ is oil density; $p_o$ is the oil pressure; $\mu_o$ is the dynamic viscosity of oil and $k_{r,o}$ is the oil relative permeability which depends on the oil saturation degree $S_{r,o} = 1 - S_{r,w}$

The oil balance equation is given by the relation:

$$\frac{\partial}{\partial t} f_o^* + div\left(\rho_o.\underline{f}_o\right) = 0 \quad (37)$$

And the oil storage is defined by:

$$f_o^* = \rho_o.n.S_{r,o} \quad (38)$$

The oil density is depending on oil pressure according to a relationship similar to equation (35).

## 3 WATER-FLOODING TEST MODELING

The water-flooding test performed on Lixhe chalk initially saturated by Soltrol™ (Schroeder & al. 1998) allows validating the developed model.

### 3.1 *Description*

The sample with an initial porosity $n$ = 40.55 % and permeability $k_{int}$ = 1mDarcy has dimensions of 25 mm of diameter and 50 mm of height. Four strain gauges are glued on the sample (located respectively from the injection side at a distance of 4, 12, 22 and 30 mm), which aims to monitoring the evolution of the axial deformation with the waterfront. In addition, an axial LVDT records the global axial deformation.

The initial stress state is isotropic at a level of 18 MPa, just below the expected pore collapse for 'oil-like' plug. The injection water pressure is equal to 0.9 MPa. Just before the injection front, a small swelling is measured by the strain gauges but a brutal and quasi-instantaneous compaction appears at the waterfront. The final amplitude of the compaction is around 2%-3%.

### 3.2 *Parameters of the model*

Experiment results of triaxial tests on saturated samples allow us to define the yield surface of oil-like and water-like plugs. The transition between these two cases is characterized by results of suction controlled oedometer tests. The parameters of the mechanical model are presented in Table 1.

Table 1. Parameters of the Cap model

| | Parameter | Value | Unit |
|---|---|---|---|
| Non linear Elasticity | | | |
| | $\kappa$ | 0.0085 | - |
| | $\nu$ | 0.2 | - |
| Frictional mechanism | | | |
| | $\phi_{water}$ | 25 | ° |
| | $\phi_{oil}$ | 25 | ° |
| | $c_{water}$ | 1.5 | MPa |
| | $c_{oil}$ | 2.0 | MPa |
| | k | 0.167 | - |
| CamClay + suction LC | | | |
| | $p_{o,water}$ | 12 | MPa |
| | $p_{o,oil}$ | 18 | MPa |
| Hardening rule | | | |
| | $\lambda(0)$ | 0.18 | - |
| | $r$ | 0.95 | - |
| | $\beta'$ | 8.0 | $MPa^{-1}$ |
| | $p_c$ | $3.\ 10^{-3}$ | MPa |

The porosimetric curve of Lixhe chalk allows to determine the retention curve (see Delage & al. 1995 for the method). The following expression is proposed:

$$S_{r,w} = \frac{CSR3}{\pi}arctan\left(-\frac{s+CSR2}{CSR1}\right)+\frac{CSR3}{2} \quad (39)$$

Where CSR1, CSR2, and CSR3 are soil constants with values CSR1 = 100 kPa; CSR2 = -325 kPa and CSR3 = 1.

It should be mentioned that this curve is defined for drying paths. However, waterflooding involves rather wetting paths. Moreover, during a waterflooding test, water drives out the oil present in the pores but a residual quantity of oil (about 30%) remains in the sample. This corresponds to the well-known hysteretic phenomenon. To match this experimental result, some numerical modifications are necessary, giving rise to another retention curve defined by the following parameters:
CSR1 = 1.0 $10^5$ Pa; CSR2 = -9.50 $10^4$ Pa and CSR3 = 0.75 for wetting path.

Generally in unsaturated soils, the relative permeability is supposed to be a function of the saturation degree. The following expressions are used in order to fit experimental relative permeability curves:

$$k_{rel,oil} = \left(1-S_e\right)^2.\left(1-S_e^{5/3}\right) \quad (40)$$

$$k_{rel,water} = \frac{\left(S_{r,w} - S_{res}\right)^6}{\left(S_{r,field} - S_{res}\right)^6} \quad (41)$$

where

$$S_e = \frac{S_{rw} - S_{res}}{S_{r,field} - S_{res}} \quad (42)$$

is the effective saturation, $S_{res}$ is the residual saturation and $S_{r,field}$ is the field saturation.

The experimental curve fitting gives $S_{res}$ = 0.01; $S_{r,field}$ = 1.

### 3.3 *Numerical Simulations*

The modelling of the waterflooding test needs the definition of the initial and boundary conditions.

- Initial conditions: the oil pressure is fixed at 100 kPa but the water pressure is unknown. As the sample is quite oil saturated, the initial suction may be estimated using the retention curve. If an initial suction of 3 MPa is chosen, it corresponds to a water pressure equal to –2.9 MPa and water saturation equal to 1.23%.The initial total stress state is isotropic at a level of 18 MPa.
- Boundary conditions: at the bottom of the sample, the water pressure is brought to 0.9 MPa. The oil can go out the sample at the upper part where oil pressure is fixed at 100 kPa. The boundary condition for the water at top of the plug is difficult to define: if the boundary is considered as impervious, no water goes out of the sample even if the water front reaches the top; if the water pressure is fixed at the top, the pressure will remain at the initial value. A specific boundary element was developed for this problem: the boundary is impermeable when the pressure is lower than a given value. In our case, the value corresponds to the atmospheric pressure.

The comparison of the numerical results with the experimental data is shown in Figure 2. The injected water volume evolution is similar. After 3500 sec, the waterfront reaches the top; no more oil is driven out of the sample and water is produced at the top. The computed axial strains at the four gauges present a small swelling followed by a brutal collapse of around 2.5% (Figure 3).

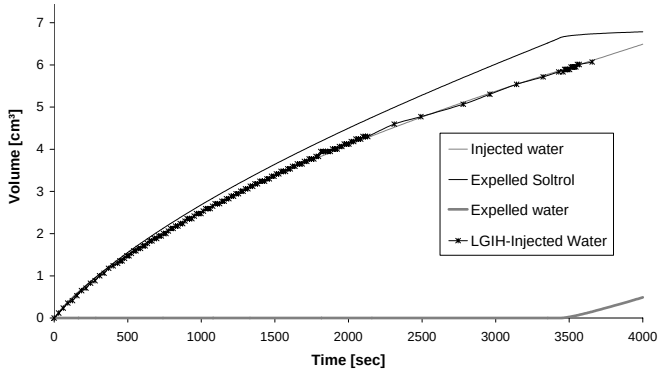


Figure 2: Fluid exchange during water flooding

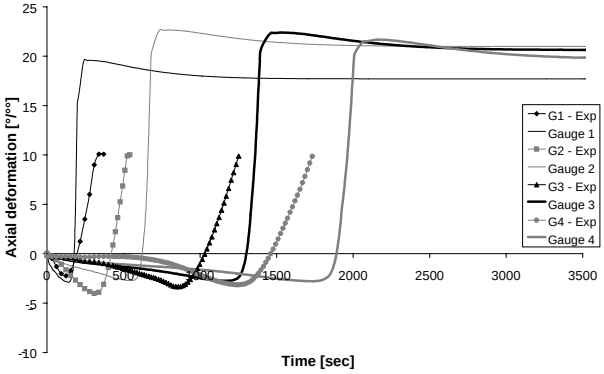


Figure 3: Axial strains at the four gauges

The experiment value of strain stops at 1%, which corresponds to the gauge failure.

The good consistence obtained between the numerical simulation and the experimental responses shows the validity of the developed model for describing the chalk behaviour during water injection.

## ACKNOWLEDGMENTS

The authors are grateful to the FNRS, the European Union and to the Communauté Française de Belgique for their financial support to this research project.

## REFERENCES

Alonso, E.E. Gens, A. & Josa, A. 1990. *A constitutive model for partially saturated soils. Géotechnique* 40(3): 405-430.

Bear, J. 1972. *Dynamics of fluids in porous media. American Elsevier Environmental science series 1972.*

Collin, F. Li, X.L. Radu, J.P. & Charlier, C. 2001. *Thermo-hydro-mechanical couplings in clay barriers. Engineering Geology. Accepted 2001.*

Delage, P. Audiguier, M. Cui, Y.J. & Deveughele, M. 1995. *Water retention proprieties and microstructure of various geomaterials. Proceedings of the 11th ECSMFE, Copenhague, Vol. 3, pp. 43-48.*

Delage, P. Schroeder, C. & Cui, Y.J. 1996. *Subsidence and capillary effects in chalk. Proc. Eurock 96, Turin 1996*: 1291 – 1298.

Monjoie, A. Schroeder, C. Prignon, P. Yernaux, C. da Silva, F. & Debande, G. 1990. *Establishment of constitutive laws of chalk and long term tests. Proc. 3rd Sea Chalk Symposium, Copenhagen June 1990.*

Schroeder, C. Bois, A.P. Maury, V. & Hallé, G. 1998. *Water/chalk (or collapsible soil) interaction: Part II. Results of tests performed in laboratory on Lixhe chalk to calibrate water/chalk models. SPE/ISRM Eurock'98 Trondheim (SPE 47587) 1998.*

Simo, J.C. & Taylor, R.L. 1985. *Consistent tangent operators for rate-independent elastoplasticity. Computer Method in Applied Mechanics and Engineering* 48:101-118.

Simo, J.C. & Hughes, T.J.R. 1998. *Computational Inelasticity. Interdisciplinary applied mathematics,* 7:198-218.

Van Eekelen, H.A.M. 1980. *Isotropic yield surfaces in three dimensions for use in soil mechanics. International Journal for Numerical and Analytical Methods in Geomechanics* 4:98-101.